

# UCLA

## UCLA Previously Published Works

### Title

The future of hybrid imaging—part 2: PET/CT

### Permalink

<https://escholarship.org/uc/item/3vn641ft>

### Journal

Insights into Imaging, 2(3)

### ISSN

1869-4101

### Authors

Beyer, Thomas  
Townsend, David W  
Czernin, Johannes  
et al.

### Publication Date

2011-06-01

### DOI

10.1007/s13244-011-0069-4

### Copyright Information

This work is made available under the terms of a Creative Commons Attribution-NonCommercial License, available at <https://creativecommons.org/licenses/by-nc/4.0/>

Peer reviewed

## The future of hybrid imaging—part 2: PET/CT

Thomas Beyer · David W. Townsend ·  
Johannes Czernin · Lutz S. Freudenberg

Received: 1 October 2010 / Revised: 14 November 2010 / Accepted: 13 January 2011 / Published online: 20 February 2011  
© The Author(s) 2011. This article is published with open access at Springerlink.com

**Abstract** Since the 1990s, hybrid imaging by means of software and hardware image fusion alike allows the intrinsic combination of functional and anatomical image information. This review summarises the state-of-the-art of dual-modality imaging with a focus on clinical applications. We highlight selected areas for potential improvement of combined imaging technologies and new applications. In the second part, we briefly review the background of dual-modality PET/CT imaging, discuss its main applications and attempt to predict technological and methodological improvements of combined PET/CT imaging. After a decade of clinical evaluation, PET/CT will continue to have a significant impact on patient management, mainly in the area of oncological diseases. By adopting more innovative

acquisition schemes and data processing PET/CT will become a fast and dose-efficient imaging method and an integral part of state-of-the-art clinical patient management.

**Keyword** Hybrid imaging · PET · CT · PET/CT

### Background and reasoning

The proposal to combine PET with CT was made in the early 1990s by Townsend, Nutt and co-workers. In addition to intrinsic image alignment, the anticipated benefit of a PET/CT hardware combination was to use the CT images to derive the PET attenuation correction factors [1]. The first prototype PET/CT became operational in 1998 [2], designed and built by CTI PET Systems in Knoxville, Tenn., USA (now Siemens Healthcare) and clinically evaluated at the University of Pittsburgh. The design incorporated a single-slice spiral CT (Somatom AR.SP; Siemens Medical Solutions, Forchheim, Germany) and a rotating ECAT ART PET system (CTI PET Systems, Knoxville, Tennessee). Torso imaging using the prototype PET/CT took 1 h, or more. Over 300 cancer patients were imaged on the prototype. The results from the prototype demonstrated the importance of high resolution anatomy accurately co-registered to functional data [3–5]. This helped localise functional abnormalities and clarified equivocal situations, thus improving the accuracy and confidence of the data interpretation. The use of rapidly acquired, low-noise CT data in place of a lengthy conventional PET transmission acquisition reduced the overall duration of the examination [6].

Unknown to the development team of the above prototype PET/CT, which served as a key impulse for the subsequent commercialisation of PET/CT development,

---

“The future belongs to those who prepare for it today” (Malcolm X).

T. Beyer (✉)  
cmi-experts GmbH,  
Pestalozzistr. 3,  
8032, Zürich, Switzerland  
e-mail: thomas.beyer@cmi-experts.com

T. Beyer · L. S. Freudenberg  
Department of Nuclear Medicine, University Hospital Essen,  
Essen, Germany

D. W. Townsend  
Singapore Bioimaging Consortium 11,  
Biopolis Way, #02-02 Helios,  
Singapore 138667, Singapore

J. Czernin  
Department of Molecular and Medical Pharmacology,  
David Geffen School of Medicine, UCLA,  
Los Angeles, CA, USA

L. S. Freudenberg  
Department of Nuclear Medicine,  
ZRN Grevenbroich, Germany

another team at Gunma University in Japan had proposed a combination of a full-ring PET and CT as early as 1984. Their design was based on the two tomographs placed next to each other with a patient handling system traversing between the two units. However, this original work was not widely known, and was not further developed towards a commercial product.

The first commercial PET/CT to be announced was the Discovery LS (GE Healthcare) in early 2001. This was followed a few months after by the Biograph (Siemens Medical Solutions), and then somewhat later by the Gemini (Philips Medical Systems). Over the years, PET/CT designs from all vendors have evolved following the advances in CT and PET instrumentation (Fig. 1). Today, six vendors

worldwide offer over 20 different PET/CT designs. All PET/CT systems permit multi-bed, whole-body imaging within a single examination, using the CT for attenuation and scatter correction of the PET data, as a prerequisite to quantitative metabolic imaging [7].

PET/CT imaging has rapidly emerged as an important imaging tool in oncology [8]. The success of PET/CT imaging is based on several factors. First, patients benefit from a comprehensive diagnostic anatomical and functional whole-body survey in a single session. Second, PET/CT provides more accurate diagnostic information than PET or CT alone. Third, PET/CT imaging allows radiation oncologists to use the functional information provided by PET for radiation treatment planning.

**Fig. 1** **a** Selected PET/CT designs offered by GE Healthcare, Philips Healthcare Systems, Siemens Healthcare Solutions, Toshiba, Hitachi and Mediso. **b** Selected system design parameters for the PET/CT systems in **a**



## Main applications

There is, at least for oncology, a growing body of literature that supports the accuracy of staging and restaging with PET/CT compared with either CT or PET acquired separately [8–10]. These improvements are incremental compared with PET, which alone demonstrates high levels of sensitivity and specificity for a wide range of disease states. Improved accuracy in primary diagnosis, staging and restaging has been documented for a variety of cancers, including head and neck, thyroid, lung, breast, oesophageal, colorectal, lymphoma, sarcoma, gastrointestinal stroma tumour (GIST), carcinoma of unknown primary, and melanoma [8, 11–13]. In summary, therefore, the improvement in accuracy of PET/CT compared with PET or CT alone for staging and restaging is statistically significant and averages 10–15% over all cancers [8].

An application on which PET/CT is also having an impact is that of radiotherapy treatment planning [14]. In anticipation of application to radiotherapy treatment planning, the patient port on early PET/CT designs was increased to 70 cm in diameter. From the beginning, PET/CT provided more convenient and routine access to fused CT and PET images and early assessment of the consequences of using PET/CT in planning [15] was encouraging. As suggested, the convenience of having fused CT and PET images for every patient immediately following the PET/CT could not be matched by even the most sophisticated software. Increasingly, PET/CT systems are being acquired by radiation oncology departments and PET images are contributing directly to the definition of treatment volumes on CT-based plans [16, 17]. This will continue to be an area of growth, particularly in meeting the demands of intensity-modulated radiation therapy (IMRT) and the availability of radiation therapy devices able to treat tumours with surgical precision using sophisticated robotic techniques. Access to other PET biomarker mapping processes, such as hypoxia [18], that increase the radio-resistance of tumours could potentially expand the role of PET in radiation oncology. First PET/CT systems dedicated to PET-guided radiation therapy planning are on the market and, with a patient port diameter of 78–85 cm, facilitate the imaging of patients in the treatment position [19, 20].

As with radiation therapy planning, PET was already finding a role in assessing therapy response before the introduction of PET/CT. A detailed discussion of the use of PET/CT for monitoring therapy response may be found elsewhere [21]. The combination of CT and PET for monitoring response offers a number of unique possibilities in spite of the technical difficulties associated with CT-based attenuation correction. First, the anatomical and functional volume of the tumour can be estimated, the

former from CT measurements and the latter by summing all voxels with standardized uptake value (SUV) [22] above a threshold that defines malignancy. Therapy response can be assessed from changes in both these metrics or from a change in the total lesion glycolysis that is calculated as the product of the average SUV in the tumour and the volume [23].

Combined PET/CT gains importance for individualised treatment planning before radionuclide therapy, which is increasingly used as a treatment technique for a range of cancers, e.g. with radiolabelled peptides [24]. To date, few treatments involve the use of dosimetry, either to plan treatment or to ascertain the delivered dose during treatment. Further, the correlation between the absorbed dose and the biological effect has been difficult to establish. PET is the most accurate imaging method for the determination of activity concentrations *in vivo*. PET imaging can be considered for pre-therapeutic treatment planning but ideally requires the use of a radioisotope from the same element as that used for treatment (e.g.  $^{124}\text{I}$  for  $^{131}\text{I}$ ;  $^{86}\text{Y}$  for  $^{90}\text{Y}$ ). For example,  $^{124}\text{I}$ -PET/CT dosimetry has emerged as a valuable tool for confirming or revising staging and for planning therapy in differentiated thyroid cancer [25–29]. Some groups proposed to routinely perform this procedure before the first radioiodine therapy (RIT) with  $^{131}\text{I}$  for thyroid remnant ablation in differentiated thyroid cancer (DTC) patients at high risk of persistent disease, i.e., patients with tumour invasion of the perithyroidal soft tissue, histologically proven lymphatic involvement, distant metastases, unfavourable histotypes, or age  $\leq 18$  years [30].

The rationale is to detect patients with previously occult loco-regional or distant metastases who may benefit from RIT with an individually tailored escalated activity. These patients receive such RIT when lesion uptake in the dosimetry procedure permits reasonably high confidence that the RIT will yield tumour doses exceeding 100 Gy, while staying within established limits for avoiding bone marrow toxicity. Patients without sufficient tumour uptake in the dosimetry procedure still receive RIT with a standard activity for remnant ablation according to national guidelines. In patients given RIT for metastatic involvement,  $^{124}\text{I}$ -PET/CT dosimetry is repeated before subsequent courses of RIT. This concept can serve as a matrix for other radionuclide therapies [31].

Since the development in CT has been driven primarily by cardiology demands for faster acquisitions, the top-of-the-line PET/CT now incorporates 128-slice CT and is in principle ideally suited to cardiac PET/CT. The ability to image both structure and function could, for example, enhance the characterisation of atherosclerotic plaques by imaging the inflammatory process associated with the plaque. The combination of CT angiography together with

a measurement of myocardial perfusion using a PET tracer such as  $^{82}\text{Rb}$ -rubidium or  $^{13}\text{N}$ -ammonia could, in a single examination, assess both the integrity of the cardiac arteries and the metabolic consequences for the myocardium [32].

Cardiac PET/CT applications are still in their infancy and have recently encountered a number of difficulties. Obviously, the effects of cardiac and respiratory motion are critical for these studies. The problems of mismatch associated with CT-based attenuation correction are potentially more serious for cardiac studies than they are for oncology, in that all cardiac studies will be affected rather than just those whole-body studies with lesions in certain sensitive regions such as the lung. This mis-registration results in what appears to be perfusion deficits in segments of the heart associated with the misalignment.

A number of different strategies are being developed to address this issue, including (1) manual realignment of CT and PET, (2) acquiring a cine CT of the breathing motion and generating an average CT for attenuation correction and (3) acquiring multiple CT data sets to ensure at least one matches the PET image as closely as possible. Obviously, the role of PET/CT in cardiology has yet to be determined, but if a strong clinical demand exists it is to be expected that transient technical challenges such as the misalignment issue will ultimately be resolved.

### Improvements and new applications

The main objective of PET is to detect metabolic abnormalities, synonymous with disease (or responses to functional tests) and to quantify these changes in metabolic uptake patterns with respect to normal background activities. Therefore, the diagnostic accuracy of PET is not only dependent on spatial resolution but, more so, on the sensitivity of the detection system. PET sensitivity describes the ability of the PET system to utilise a fraction of the injected activity for signal detection. The higher the sensitivity, the more signal is detected for a given activity injected, thereby providing increased detectability of lesions.

PET is intrinsically a three-dimensional (3D) imaging methodology, replacing physical collimation required for single-photon imaging with the electronic collimation of coincidence detection. The availability of PET systems with retractable inter-plane septa encouraged the use of 3D methodology, at least for the brain, where the net increase of a factor of 5 in sensitivity could be realised [33]. The situation for whole-body imaging is far less favourable, in part due to the presence of significant activity just outside the imaging field of view (FOV) in most bed positions. With the

appearance of LSO (lutetium oxyorthosilicate)- and GSO (gadolinium silicate)-based PET, which could be operated with short coincidence time windows (4.5–6 ns) and higher lower-energy thresholds (400–450 keV) compared with 10–12 ns and 350 keV for a typical BGO-based PET, significantly improved whole-body image quality has been achieved in 3D [34].

The sensitivity of a PET system can also be improved by the addition of more detector material. Planar sensitivity can be increased by extending the thickness of the scintillator (Fig. 2). In this example, a 50% increase in thickness from 20 mm to 30 mm results in a 40% increase in sensitivity. However, increasing the axial extent by 33% will result in a 78% increase in volume sensitivity (for 3D acquisition with no septa). The latter thus makes more efficient use of the increased volume of the scintillation detector material, although there will also be an increase in the number of phototubes required (and hence increased cost). Following an injection of a radioactive tracer such as 2-deoxy-2- $(^{18}\text{F})$ fluoro-D-glucose (FDG), the patient receives a radiation dose from all annihilation photons, not just those emitted within the imaging FOV of the PET system. Therefore, the greater the axial coverage, the better use is made of the radiation emitted and the more efficient use is made of a given volume of scintillator. For most PET/CT, axial PET coverage is about 16 cm. The most recent design announced has an extended FOV covering 21.8 cm axially.

Despite the increase in volume sensitivity from increased axial coverage (Fig. 2), 3D PET suffers from a sharp decrease in sensitivity at both ends of the axial FOV. This drop in sensitivity mandates slightly overlapping bed positions when imaging larger imaging fields, such as the torso or the whole-body. Sensitivity in the overlapping regions is slightly lower than the sensitivity in the centre of the axial FOV. Dahlbom and co-workers suggested as early as 1992 a continuous axial sampling mode by moving the patient bed in steps equal to half the plane separation [35]. As a result, better image uniformity and sensitivity was achieved, together with a reduction in noise compared with standard multi-bed acquisition modes. Further refinements of the continuous acquisition mode for PET were suggested by the same authors [36]. However, the improvements in clinical image quality were less obvious than in simulation studies. Nonetheless, continuous bed motion based on modern hardware and highly accurate bed positioning and position tracing should yield a significant improvement in whole-body PET image quality. Continuous PET acquisition would then be complementary to continuous, spiral CT acquisitions as performed in PET/CT. Finally, continuous bed motion supports the free definition of co-axial imaging ranges that otherwise would be limited by an integer number of PET bed positions, and, thus, lead to an

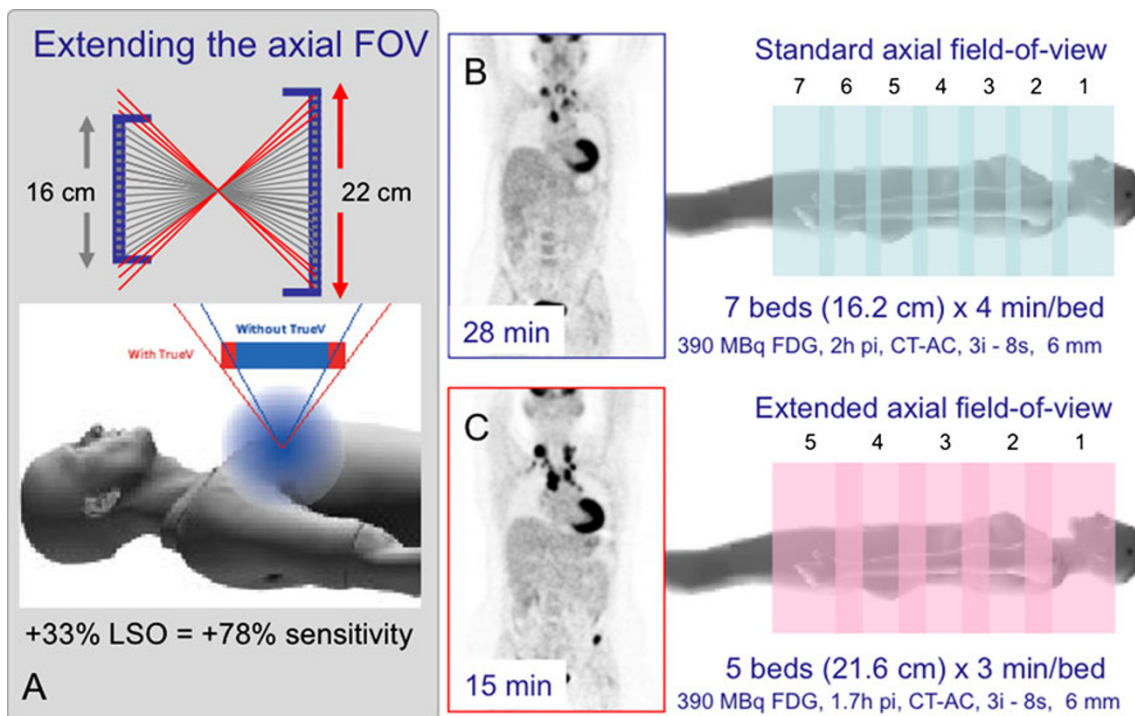


**Fig. 2** **a** Improving the sensitivity of a PET system by increasing the axial length of the tomograph from 16 cm to 22 cm. **b, c** Increased volume sensitivity can be used to reduce overall imaging time by acquiring fewer bed positions. (With source information from Siemens Healthcare)

overexposure of the patients in the lower part of the co-axial imaging range.

In order to increase lesion detectability in PET, spatial resolution must be improved as well. This is achieved by making crystal detectors smaller [19]. However, infinitesimally small PET detectors are not feasible as the volume sensitivity would be much reduced. Therefore, improved spatial resolution must be optimised with respect to volume sensitivity. Most PET/CT systems today offer 4-mm crystals that are 20-mm deep (Fig. 3). By making PET detectors smaller spatial resolution is improved and, for example, smaller-sized, active lymph nodes can be better detected, the main parameter for lesion detection in PET being the activity concentration (or lesion-to-background contrast) notwithstanding. This is of the essence, considering that a significant number of normal-sized lymph nodes in oncology patients harbour disease, as is known from the sentinel lymph node experience in breast cancer [37] or from patients with lung cancer [38].

While most PET and PET/CT systems offer isotropic resolution, this is true only for the central FOV. Spatial resolution deteriorates in the transverse direction towards the edge of the FOV, i.e. the detector ring, because of increased depth-of-interaction effects. This is illustrated in Fig. 4. Spatial resolution can be recovered particularly in these regions by measuring a point source at given locations of the FOV and by incorporating a spatially variant point spread function (PSF) model into the iterative

reconstruction process [39]. The resulting image quality is much improved and spatial resolution is made more uniform throughout the FOV.

Co-registered CT images may also be used to improve partial volume correction by dividing the standardised uptake value (SUV) from the PET image with a recovery coefficient based on the spherical tumour diameter. As tumours generally have a complex shape, a more sophisticated partial volume correction method is desirable [40]. Thus, for both technical and practical reasons, PET/CT is continuing to successfully promote the use of PET for monitoring response to different forms of therapy.

The availability of fast scintillators with high stopping power such as LSO (and LYSO) has revived interest in PET time-of-flight (TOF) [41, 42], interest that has been further stimulated by the first commercial PET/CT with TOF—the Philips Gemini TrueFlight [43, 44]. The principle of TOF PET is illustrated schematically in Fig. 5: photons travel at the speed of light,  $c$ , and, therefore, one of the annihilation photons will arrive at the detector with a time-delay of  $2\Delta/c$ , where  $\Delta$  is the distance of the positron–electron annihilation from the axis of the tomograph. This information is incorporated into the reconstruction process. Theoretical arguments lead to a possible increase in the signal-to-noise ratio (SNR) proportional to  $\sqrt{D/\Delta d}$ , where  $D$  is the patient diameter and  $\Delta d$  the uncertainty of the location of the annihilation. Thus, the advantage of TOF is more significant in heavier patients, where image quality in general is worse

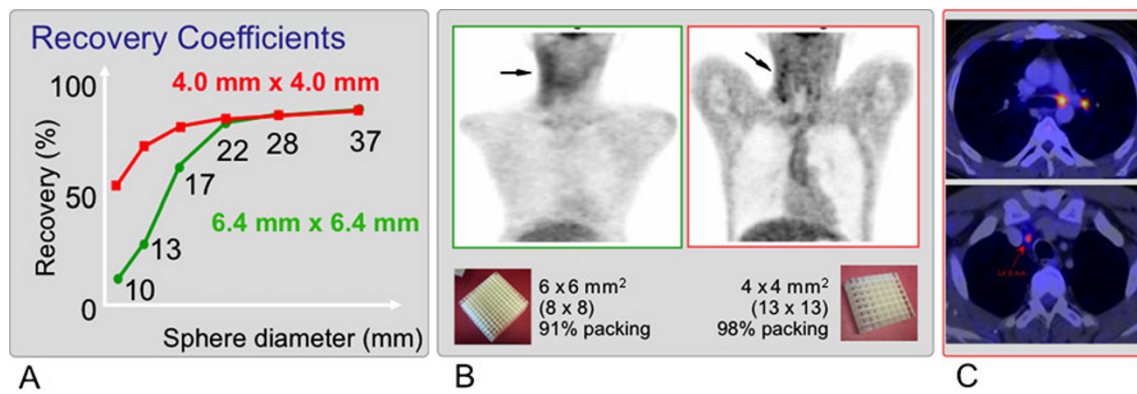


**Fig. 3** **a, b** Spatial resolution of PET is improved by making PET detectors smaller. Smaller detectors (**b**) and increased recovery (**a**) help recover small lesions, such as active lymph nodes that are normal size on CT (**c**)

compared with smaller-sized patients because of higher attenuation and scatter contributions.

The PET systems with fast scintillators and electronics can measure this time difference within a certain resolution. For example, for a PET system with a coincidence timing resolution of 500 ps, the spatial uncertainty on the position of the annihilation is 7.5 cm. For a 40-cm diameter uniform distribution and a 7.5-cm uncertainty, the increase in SNR is a factor of about 2.3. As the TOF resolution improves, the spatial uncertainty decreases and the SNR increases by a larger factor. TOF PET systems must demonstrate good

timing resolution that is stable over time so as to avoid frequent detector recalibration [45]. While promising, the clinical impact of TOF PET has yet to be established [46, 47].

There has been significant progress during the past few years in image reconstruction methods through the introduction of statistically based algorithms into the clinical setting. Iterative reconstruction methods became of clinical interest in nuclear medicine imaging with the accelerated convergence achieved by the ordered subset expectation maximisation (OSEM) algorithm [48]. Lately iterative

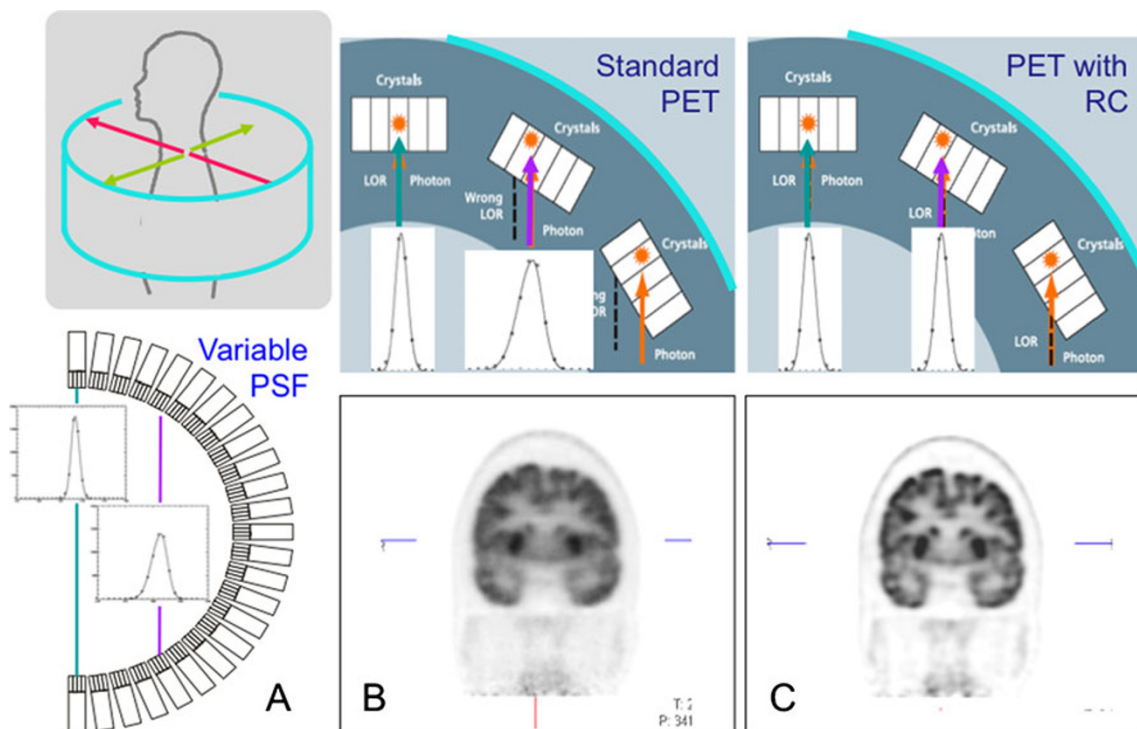


**Fig. 4** **a** Spatial resolution of PET deteriorates towards the edge of the FOV because of the increased depth-of-interaction effects (**b**). Resolution recovery (RC) is possible by measuring a standard point source throughout the FOV and deconvolving the image signal with

the spatially variant point spread function. **c** As a result, images are less noisy and spatial resolution is made more uniform, yielding an overall improved image quality. (With source information from Siemens Healthcare)

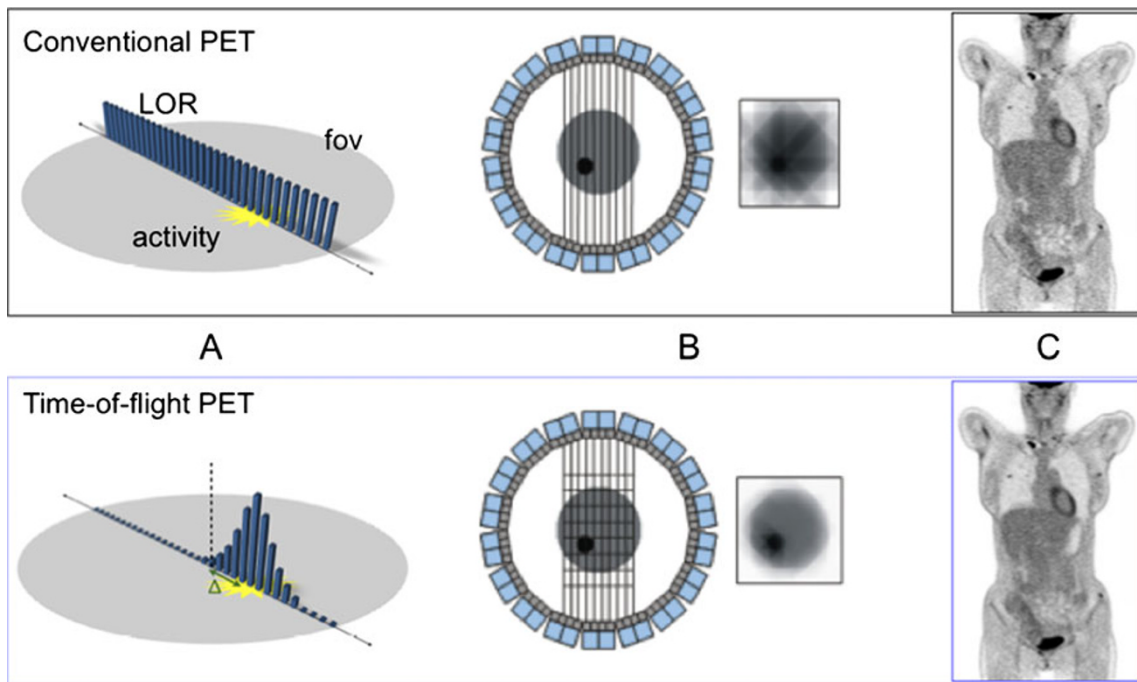


**Fig. 5** Schematic illustration of the differences between conventional PET (top) and TOF-PET (bottom). In conventional PET, there is equal probability (illustrated by the blue bars) for the recorded event along the LOR (a). In TOF-PET, the time difference between the arrival of the two annihilation photons, is used to create a probability distribution locating the recorded event at distance  $\Delta$  from the axis

of the tomography (dashed line). A timing resolution of 600 ps, for example, results in a FWHM of about 9 cm. The probability distribution and knowledge about the timing resolution of the detector system can be incorporated into the reconstruction process, illustrated here for a single projection (b). c Reconstructed PET emission images illustrate the improved SNR in TOF-PET for a patient with BMI 24

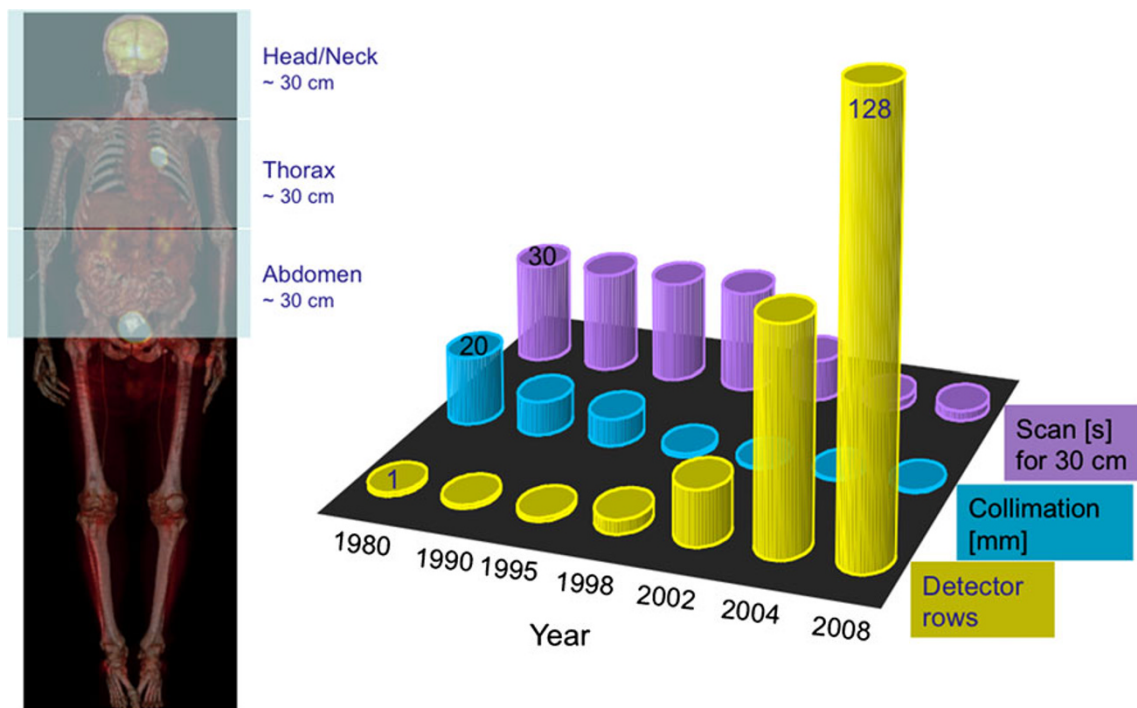


**Fig. 6** Performance of CT systems expressed as number of detector rows and measured as imaging time (s) and collimation (mm) for a typical local imaging station of 30 cm. Commercial PET/CT systems today employ CT technology with up to 128 simultaneously acquired slices



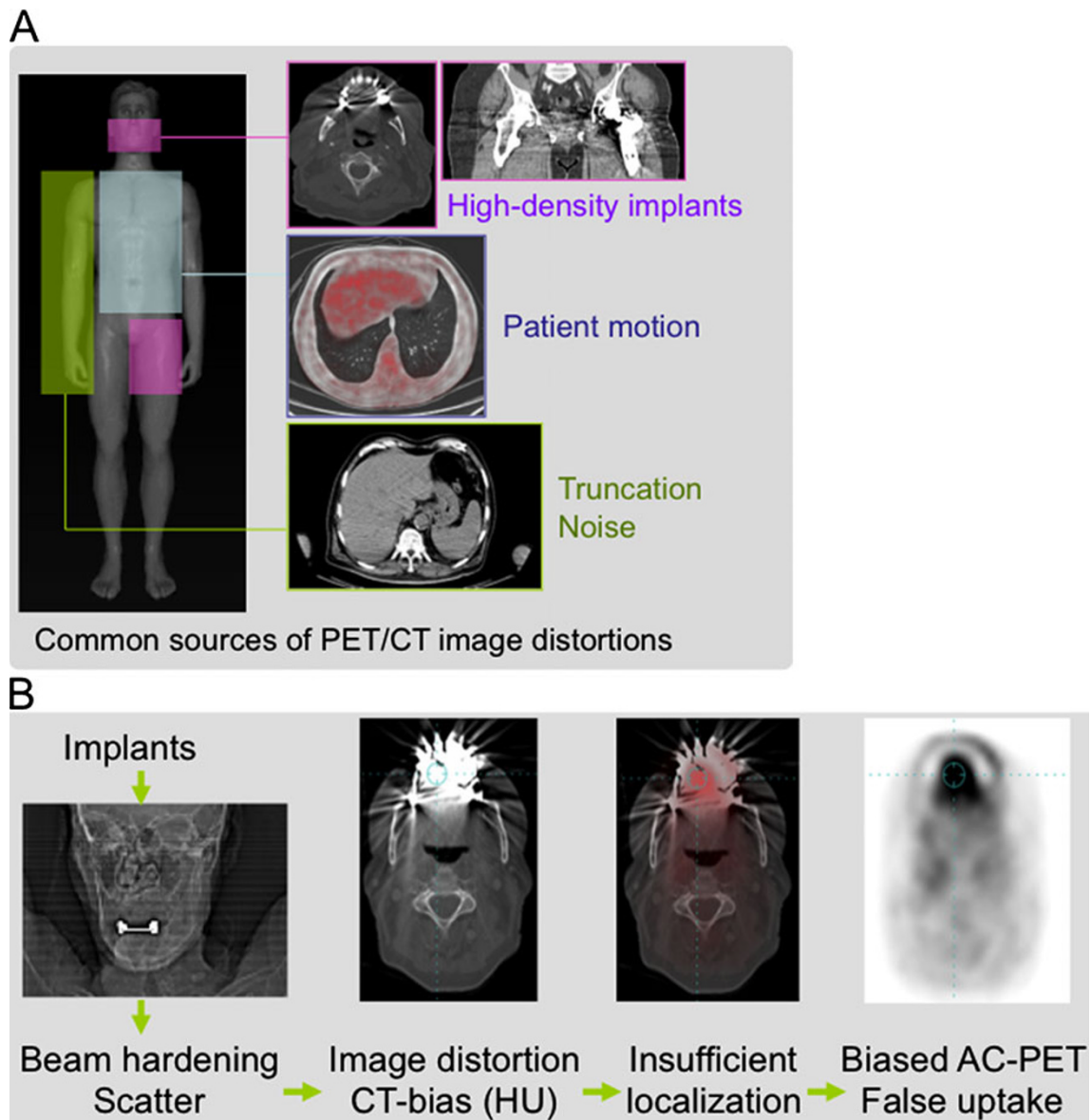


**Fig. 7** **a** Sources of PET/CT image artefacts in clinical routine imaging. **b** Metal artefacts, for example, are known to cause locally biased activity distributions on PET following CT-AC that are amplified by patient motion

image reconstruction has been proposed for clinical CT imaging as well, particularly as a method of keeping radiation exposure at low levels for an overall reduced patient exposure [49].

Further improvement can be achieved by eliminating the rebinning step and implementing OSEM fully in 3D with corrections for randoms, scatter, attenuation and detector efficiency variations incorporated into the system model [50]. Finally, in a recent development termed high-definition (HD) PET, the detector spatial response function has also been included in the reconstruction model [39]. The point spread function varies throughout the FOV owing to the oblique penetration of the detectors by annihilation photons. By measuring this variability and then modelling

the PSF, improved and near-uniform spatial resolution can be achieved throughout the FOV (Fig. 4).

All vendors provide comparable software capable of producing clinical images of high quality [7]. The greatest outstanding effect on image quality and a challenge to reconstruction algorithms is now the size of the patient, a significant problem given the current levels of obesity in industrialised countries.

After many years of slow but steady progress, the past decade has seen significant advances in both hardware and software for CT. Following the appearance of single-slice spiral CT scanners in the early 1990s [51], CT performance evolved with the advent of multi-detector arrays (MDCT), accompanied by increases in X-ray power (60 kW or greater)

and computer capacity for data processing and image reconstruction. Dual- and four-slice CT first appeared around 1998 with timing resolution of 500 ms (at 1 s rotation time), followed by 16-slice CT in 2002, 64-slice in 2004, dual-source systems in 2005, 128-slice in 2006 and 256-slice in 2006. The increasing number of detector rows (slices) and the availability of dual-source CT in combination with faster rotation times support a time resolution of 75 ms, or better (Fig. 6). Spatial resolution has improved from about 10 line pairs (Lp)  $\text{cm}^{-1}$  in 1990 to 25 Lp  $\text{cm}^{-1}$ , or better today, and with a slice thickness of less than 1 mm. However, not all kinds of CT systems are available in PET/CT or SPECT/CT combinations.

While the benefits of CT-based attenuation are now well documented, a number of challenges have emerged as the technique has become more widely adopted for PET/CT (Fig. 7). There are two main reasons for possible artefacts: (1) the presence of materials in the patient with effective atomic numbers (Zeff) that do not conform to the basic assumptions in the bi-linear transformation model [1, 52] and (2) mismatch between the CT and PET due to patient respiration, cardiac motion and bowel movement [53]. Since the first commercial PET/CT installation in 2001, these issues have received considerable attention. In most cases associated artefacts can be limited or avoided by adopting disease-specific and optimised imaging protocols [54, 55]. A thorough appreciation of clinical imaging and workflow together with some prospective training is required to implement these protocols.

However, some image artefacts must be accepted as inherent to PET/CT (and SPECT/CT) imaging. Of particular importance in the assessment of head and neck cancer is the presence of dental fillings [56] (Fig. 7b). A number of metal artefact reduction techniques have been explored in research [57, 58] but still await routine implementation in PET/CT.

Nonetheless, after a decade of clinical evaluation PET/CT continues to have a significant impact on patient management, mainly in the area of oncological diseases. Image artefacts inherent to PET/CT can be detected, interpreted and—in many cases—corrected or avoided by well-trained users. By adopting more innovative acquisition schemes and data processing PET/CT will become a fast and dose-efficient imaging method and manifest itself as an integral part of state-of-the-art patient management.

**Acknowledgements** We are indebted to Dale Bailey (Sydney), Andreas Bockisch (Essen), Claude Comtat (CEA Orsay), Bernd Pichler (Tübingen), York Hämisch (Bioscan), Matthias Hofmann (Tübingen), Ora Israel (Haifa), Antonis Kalemis (Philips London), Armin Kolb (Tübingen), Paul E Kinahan (Seattle), Thomas Krause (Bern), Roger Lecomte (Sherbrooke), Marcus Lonsdale (Copenhagen), Bernd Schweizer (Philips Research Aachen), Rainer Veigel (Philips Zurich) for helpful discussions, advice and support materials.

**Conflicts of interest** T.B. is the founder and president of Switzerland-based cmi-experts GmbH.

D.T. acts as scientific advisor to cmi-experts of Zurich, Switzerland and RefleXion Medical of Stanford, Calif., USA. He received royalty payments from Siemens Healthcare related to the invention of the PET/CT.

J.C. is co-founder of Momentum Biosciences and Sofie Biosciences, Los Angeles, Calif., USA and serves as an advisor to cmi-experts GmbH, Switzerland.

L.S.F. is an associate of ZRN Grevenbroich and Dormagen, and serves as an advisor to cmi-experts of Zurich, Switzerland. He has received speaker fees from Siemens, Philips and Genzyme.

**Open Access** This article is distributed under the terms of the Creative Commons Attribution Noncommercial License which permits any noncommercial use, distribution, and reproduction in any medium, provided the original author(s) and source are credited.

## References

- Kinahan PE et al (1998) Attenuation correction for a combined 3D PET/CT scanner. *Med Phys* 25(10):2046–2053
- Beyer T et al (2000) A combined PET/CT tomograph for clinical oncology. *J Nucl Med* 41(8):1369–1379
- Charron M et al (2000) Image analysis in patients with cancer studied with a combined PET and CT scanner. *Clin Nucl Med* 25(11):905–910
- Kluetz PG et al (2000) Combined PET/CT imaging in oncology: Impact on patient management. *Clin Positron Imaging* 3(3):1–8
- Meltzer C, Martinelli M, Beyer T (2001) Whole-body FDG PET imaging in the abdomen: value of combined PET/CT. *J Nucl Med* 42:35P
- Kinahan P, Hasegawa B, Beyer T (2003) X-ray-based attenuation correction for PET/CT scanners. *Semin Nucl Med* 33(3):166–179
- Townsend D (2008) Multimodality imaging of structure and function. *Phys Med Biol* 53(4):R1–R39
- Czernin J, Allen-Auerbach M, Schelbert H (2007) Improvements in cancer staging with PET/CT: literature-based evidence as of September 2006. *J Nucl Med* 48 (Suppl 1):78S–88S
- Hellwig D, Baum R, Kirsch C (2009) FDG-PET, PET/CT and conventional nuclear medicine procedures in the evaluation of lung cancer: a systematic review. *Nuklearmedizin* 48(2):59–69
- Ben-Haim S, Ell P (2009) 18 F-FDG PET and PET/CT in the evaluation of cancer treatment response. *J Nucl Med* 50(1):88–99
- Facey K et al (2007) Overview of the clinical effectiveness of positron emission tomography imaging in selected cancers. *Health Technol Assess* 11(44):iii–iv, xi–267
- Poeppl T et al (2009) PET/CT for the staging and follow-up of patients with malignancies. *Eur J Radiol* 70(3):382–392
- Weber W, Grosu A, Czernin J (2008) Technology Insight: advances in molecular imaging and an appraisal of PET/CT scanning. *Nat Clin Pract Oncol* 5(3):160–170
- Ford E et al (2009) 18 F-FDG PET/CT for image-guided and intensity-modulated radiotherapy. *J Nucl Med* 50(10):1655–1665
- Grosu A-L et al (2005) Positron emission tomography for radiation treatment planning. *Strahlenther Onkol* 8:483–499
- Lecchi M et al (2008) Current concepts on imaging in radiotherapy. *Eur J Nucl Med Mol Imaging* 35(4):821–837
- Dirix P et al (2009) Dose painting in radiotherapy for head and neck squamous cell carcinoma: value of repeated functional imaging with 18F-FDG PET, 18F-fluoromisonidazole PET, diffusion-weighted MRI, and dynamic contrast-enhanced MRI. *J Nucl Med* 50(7):1020–1027

18. Dehdashti F et al (2003) In vivo assessment of tumor hypoxia in lung cancer with  $^{60}\text{Cu}$ -ATSM. *Eur J Nucl Med Mol Imaging* 30(6):844–850
19. Lonsdale M, Beyer T (2010) Dual-modality PET/CT instrumentation—today and tomorrow. *Eur J Radiol* 73(3):452–460
20. Sattler B et al (2010) PET/CT (and CT) instrumentation, image reconstruction and data transfer for radiotherapy planning. *Radiother Oncol* 96:288–297
21. Weber W, Figlin R (2007) Monitoring cancer treatment with PET/CT: does it make a difference? *J Nucl Med* 48(Suppl 1):36S–44S
22. Thie J (2004) Understanding the standardized uptake value, its methods, and implications for use. *J Nucl Med* 45(5):1431–1434
23. Larson SM et al (1999) Tumor treatment response based on visual and quantitative changes in global tumor glycolysis using PET-FDG imaging: The visual response score and the change in total lesion glycolysis. *Clin Positron Imaging* 2(3):159–171
24. Cremonesi M et al (2006) Dosimetry in peptide radionuclide receptor therapy: a review. *J Nucl Med* 47:1467–1475
25. Frey P, Townsend D, Flattet A (1986) Tomographic imaging of the human thyroid using I-124. *J Clin Endocrinol Metab* 63:918–927
26. Pentlow K, Graham M, Lambrecht R (2007) Quantitative imaging of iodine-124 with PET. *J Nucl Med* 37:1557–1562
27. Erdi YE et al (1999) Radiation dose assessment for I-131 therapy of thyroid cancer using I-124 PET imaging. *Clin Positron Imaging* 2:41–46
28. Eschmann SM et al (2002) Evaluation of dosimetry of radioiodine therapy in benign and malignant thyroid disorders by means of iodine-124 and PET. *Eur J Nucl Med* 29(6):760–767
29. Jentzen W et al (2008) Optimized  $^{124}\text{I}$  PET dosimetry protocol for radioiodine therapy of differentiated thyroid cancer. *J Nucl Med* 49(6):1017–1023
30. Freudenberg L et al (2010) Lesion dose in differentiated thyroid carcinoma metastases after rhTSH or thyroid hormone withdrawal: ( $^{124}\text{I}$ ) PET/CT dosimetric comparisons. *Eur J Nucl Med Mol Imaging* 37(12):2267–2276
31. Bockisch A et al (2006)  $^{124}\text{I}$  in PET imaging: impact on quantification, radiopharmaceutical development and distribution. *Eur J Nucl Med* 33(11):1247–1248
32. Menezes L et al (2009) Assessment of left ventricular function at rest using rubidium-82 myocardial perfusion PET: comparison of four software algorithms with simultaneous 64-slice coronary CT angiography. *Nucl Med Commun* 30(12):918–925
33. Townsend DW (2004) From 3-D positron emission tomography to 3-D positron emission tomography/computed tomography: what did we learn? *Mol Imaging Biol* 6(5):275–290
34. Watson CC et al (2005) Optimizing injected dose in clinical PET by accurately modeling the counting-rate response functions specific to individual patient scans. *J Nucl Med* 46(11):1825–1834
35. Dahlbom M et al (1992) Methods for improving image quality in whole body PET scanning. *IEEE Trans Nucl Sci* 39(4):1079–1083
36. Dahlbom M, Reed J, Young J (2001) Implementation of true continuous bed motion in 2-D and 3-D whole-body PET scanning. *IEEE Trans Nucl Sci* 48(4):1465–1469
37. Cheng G et al (2010) Current status of sentinel lymph-node biopsy in patients with breast cancer. *Eur J Nucl Med Mol Imaging*. doi:10.1007/s00259-010-1577-z
38. Freudenberg L et al (2010) PET versus PET/CT dual-modality imaging in evaluation of lung cancer. *Thorac Surg Clin* 20(1):25–30
39. Panin V et al (2006) Fully 3-D PET reconstruction with system matrix derived from point source measurements. *IEEE Trans Med Imaging* 25(7):907–921
40. Soret M, Bacharach S, Buvat I (2007) Partial-volume effect in PET tumor imaging. *J Nucl Med* 48(6):932–945
41. Budinger T (1983) Time-of-flight positron emission tomography: status relative to conventional PET. *J Nucl Med* 24(1):73–78
42. Moses W (2003) Time of flight in PET revisited. *IEEE Trans Nucl Sci* 50(5):1325–1330
43. Surti S et al (2007) Performance of Philips Gemini TF PET/CT scanner with special consideration for its time-of-flight imaging capabilities. *J Nucl Med* 48(3):471–480
44. Surti S, Karp J (2009) Experimental evaluation of a simple lesion detection task with time-of-flight PET. *Phys Med Biol* 54(2):373–384
45. Daube-Witherspoon M et al (2006) Influence of the time-of-flight kernel accuracy in TOF-PET reconstruction. *IEEE MIC*. doi:10.1109/NSSMIC.2006.354230
46. Murray I et al (2010) Time-of-flight PET/CT using low-activity protocols: potential implications for cancer therapy monitoring. *Eur J Nucl Med Mol I* 37(9):1643–1653
47. Lois C et al (2010) An assessment of the impact of incorporating time-of-flight information into clinical PET/CT imaging. *J Nucl Med* 51(2):237–245
48. Hudson HM, Larkin RS (1994) Accelerated image reconstruction using ordered subsets of projection data. *IEEE Trans Med Imaging* 13:601–609
49. Flohr T et al (2010) Pushing the envelope: new computed tomography techniques for cardiothoracic imaging. *J Thorac Imaging* 25(2):100–111
50. Comtat C et al (2002) Clinically feasible reconstruction of 3D whole-body PET/CT data using blurred anatomical labels. *Phys Med Biol* 47:1–20
51. Kalender WA et al (1990) Spiral volumetric CT with single-breath-hold technique, continuous transport, and continuous scanner rotation. *Radiology* 176:181–183
52. Burger C et al (2002) PET attenuation coefficients from CT images: experimental evaluation of the transformation of CT into PET 511-keV attenuation coefficients. *Eur J Nucl Med* 29(7):922–927
53. Nakamoto Y et al (2003) Accuracy of image fusion of normal upper abdominal organs visualized with PET/CT. *Eur J Nucl Med Mol I* 30(4):597–602
54. Beyer T et al (2004) Acquisition protocol considerations for combined PET/CT imaging. *J Nucl Med* 45(Suppl 1):25S–35S
55. Beyer T, Veit-Haibach P (2006) Oncology tasks require disease-specific PET/CT. *Diagn Imaging Europe* December 2006/January 2007:14–18
56. Kamel EM et al (2003) Impact of metallic dental implants on CT-based attenuation correction in a combined PET/CT scanner. *Eur Radiol* 13:724–728
57. Schäfers K, Raupach R, Beyer T (2006) Combined  $^{18}\text{F}$ -FDG-PET/CT imaging of the head and neck. An approach to metal artifact correction. *Nuklearmedizin* 45:219–222
58. Hamill J et al (2006) A knowledge-based method for reducing attenuation artefacts caused by cardiac appliances in myocardial PET/CT. *Phys Med Biol* 51(11):2901–2918